HHS Public Access

Author manuscript

Melanoma Res. Author manuscript; available in PMC 2019 June 01.

Published in final edited form as:

Melanoma Res. 2018 June ; 28(3): 237–245. doi:10.1097/CMR.0000000000000439.

Lymphoid aggregates in desmoplastic melanoma have features of tertiary lymphoid structures

Anne M. Stowman, M.D.[1], **Alexandra W. Hickman, B.S.**[2], **Ileana S. Mauldin, Ph.D.**[3], **Adela Mahmutovic, B.S.**[3], **Alejandro A. Gru, M.D.**[4], and **Craig L. Slingluff Jr., M.D.**[3]

[1]University of Vermont Medical Center, Department of Pathology, Burlington, Vermont

[2]University of Virginia School of Medicine, Charlottesville, Virginia

[3]University of Virginia Health System, Department of Surgery, Charlottesville, Virginia

[4]University of Virginia Health System, Department of Pathology, Charlottesville, Virginia

Abstract

Background—Desmoplastic melanomas (DM) have unique and challenging clinical presentations and histomorphology. A characteristic feature is the presence of scattered lymphoid aggregates. However, the nature of these aggregates is not defined. We hypothesized that they may be tertiary lymphoid structures (TLS), and may be associated with PD-L1 expression.

Methods—We searched our tissue database for "pure" DMs and for scars as control tissues, collected clinical information, and reviewed H&E histology. We performed multispectral imaging after staining for CD8, CD20, PNAd, FoxP3, CD83, and Ki67, and assessed PD-L1 expression by immunohistochemistry (IHC).

Results—Pure DM samples were evaluable in 11 patients. All had desmoplastic stroma and lymphoid aggregates on H&E. The lymphoid aggregates of 8/11 (72%) DM samples and only 3/11 scars contained features of TLS, defined as: distinct clusters of B cells and $CD8^+$ T cells, $CD83^+$ dendritic cells in T cell zones; and $PNAd^+$ vasculature resembling high endothelial venules (HEVs). PD-L1 was expressed by ≥ 1% of melanoma cells in 6/11 and by ≥ 5% of immune cells in 10/11 DM samples.

Discussion—We found that most lymphoid aggregates in DM are organized, classical TLS. PD-L1 expression was detected in most cases, and was highest in two cases of DM with TLS. However, low PD-L1 expression in some cases suggests that some DM cells may be unresponsive to IFN-γ. TLS support antigen presentation and T cell responses in chronic inflammation and cancer. Their presence in DM likely reflects an adaptive immune response, which may be enhanced with immune therapies.

Corresponding author: Craig L. Slingluff, Jr., M.D., University of Virginia Health System, 1215 Lee Street, Department of Surgery, Charlottesville, Virginia 22908, Phone: 434-924-2129, Fax: 434-982-5959, CLS8H@virginia.edu.

Conflict of interest: None to declare

Keywords

desmoplastic melanoma; spindle cell melanoma; lymphocytes; tertiary lymphoid structure; B-cells; T-cells

Introduction

Desmoplastic melanoma (DM) is a subtype of spindle cell melanoma with a distinct clinical presentation and unique histologic features. It classically presents on sun-exposed skin of the head and neck as a nonpigmented nodule or plaque in older adults. Histologically, the tumors are characterized by three key features: 1) a lentiginous melanocytic proliferation along the dermoepidermal junction, 2) a dermal spindle cell population set within desmoplastic stroma, and 3) intratumoral lymphoid aggregates. The dermal component is often subtle, and in 20–30% of cases, an intraepidermal component is absent, contributing to the diagnostic challenge [1–3]. Thus, especially in these cases, lesions of DM can be confused with fibrosis or scar and misdiagnosed [3,4]. Most characteristic and helpful to the identification of DMs are the desmoplastic stroma and lymphoid aggregates. Intriguingly, the composition of these lymphoid aggregates of DMs have yet to be characterized. We hypothesized that the aggregates may be tertiary lymphoid structures (TLS).

Secondary lymphoid structures (lymph nodes and spleen) exist in well-defined areas, and have critical roles in adaptive immunity. However, lymphoid tissue can arise de novo in other tissues by a process termed lymphoid neogenesis [5], giving rise to TLS, which have features that resemble lymph node tissues. Specifically, TLS are characterized by discrete T and B cell zones, mature dendritic cells within the T cell zone, and specialized blood vessels with features of high endothelial venules (HEVs) [5–8]. While structures with all three of these features have been termed by some as “classical” TLS [9], the heterogeneity of structures identified in some human cancers has led to the broader definition of “non-classical” TLS—i.e., lymphoid aggregates that share some but not all of the three primary defining characteristics [10]. TLS, also referred to as tertiary lymphoid organs (TLOs), or tumor-localized ectopic lymph node-like structures (TL-ELNs), have been identified in areas of chronic inflammation [11,12], as well as in multiple solid tumors [13–15], including conventional melanomas [16,17] and their metastases [18]. In inflamed non-lymphoid tissues, TLS can support the inflammation or autoimmune reactivity [5]. In cancers, the presence of TLS has been associated with tumor-infiltrating lymphocytes (TIL) [14], and with favorable clinical outcomes, attributed to local and/or systemic antitumor T and B cell responses [9,12]. To this end, we hypothesized that the lymphocytic aggregates seen in DMs are part of a chronic adaptive immune response, and anticipated to find features of TLS formation, including discrete $CD20^+$ B cell areas, $CD83^+$ dendritic cells within the T cell zone, and $PNAd^+$ vasculature.

DM has been associated with an extremely high mutational burden [19]; thus, multiple studies have speculated that immunotherapy may be of particular benefit in this subset of patients [20,21]. The interaction of programmed death 1 (PD1) on T cells with the programmed death ligand 1 (PD-L1) inhibits the anti-tumor $CD8^+$ cytotoxic T cell response.

PD-L1 expression is enhanced by IFN-γ [22]. and is often localized in tumor tissues near TIL [23,24]. We hypothesized that if the TLS in DM contain activated T cells producing IFN-γ, PD-L1 expression would be near the TLS. We quantified PD-L1 expression in our samples to study the association with the presence or absence of TLS.

Methods

With IRB approval (IRB #19694), we searched our database for cases of “pure” DM between the years 1995–2016. We defined “pure” DM as those cases in which the infiltrate was predominantly dermal-based, paucicellular, and composed of atypical spindled cells set within a desmoplastic or sclerotic stroma with evidence of melanocytic differentiation [25–27]. We identified 23 cases biopsied at our institution; of those, 12 had materials available for review and study, of which 11 were evaluable on multicolor histology. Patient age, sex, biopsy site and procedure were recorded from the pathology report. We reviewed the hematoxylin and eosin (H&E) slides and IHC stains.

As this study was initiated to explore the histopathological diagnostic challenges of DM, cases of “scar” were selected as our controls. We retrieved 12 cases of scar, 11 of which were evaluable. They included re-excision specimens after squamous cell carcinoma (1), basal cell carcinoma (1), melanomas in situ (2), or atypical nevi (1). The remaining cases were as follows: wide excision for a melanoma (1); scar revision status post Mohs surgery (2); scar collected from an open repair of a recurrent abdominal hernia (1); repair of a chronic wound (1); and a clinically suspicious papule found to be scar (1). We reviewed the H&E slides for diagnosis and presence of inflammation.

Three 4-μm thick sections were cut of each specimen; one section of tonsil and lymph node were cut for positive and negative controls. The slides for multispectral imaging analysis were prepared by the Opal Multiplex Manual IHC Kit (PerkinElemer, Waltham, MA) for immunofluorescent (IF) staining on the PerkinElmer Vectra 3.0 system. Staining was performed according to the manufacturers protocol; however, slides were allowed to cool for 30 min at room-temperature post-microwaving in antigen retrieval (AR) buffer, and to facilitate continuation of staining, were stored overnight in AR buffer at 4 degrees Fahrenheit. AR for the FoxP3 stain was performed using Diva Decloaker (Biocare Medical, Concord, CA). Staining sequence, antibodies, and antigen retrieval buffers were as follows: AR9 CD8 (dilution 1:500, Dako, Santa Clara, CA) Opal540; AR6 CD20 (1:1000, Dako) Opal520; Diva Decloaker FoxP3 (1:500, Cell Signaling Technology, Danvers, MA) Opal570; AR6 PNAd (1:1000, BD Biosciences, Franklin Lakes, NJ) Opal620; AR6 CD83 (1:200, Santa Cruz Biotechnologies, Dallas, TX) Opal650; AR6 Ki67 (1:20, Abcam, Cambridge, MA) Opal 690. Slides were mounted using prolong diamond antifade (Life Technologies, Carlsbad, CA) and scanned at 10× using the PerkinElmer Vectra 3.0 system and Vectra software. The images obtained at 10× were spectrally mixed. Regions of interest were then identified in Phenochart (PerkinElmer, Hopkinton, MA), and a 20× image was acquired. These images were spectrally unmixed using a single stain positive control, and analyzed using the InForm software (PerkinElmer, Hopkinton, MA).

Staining performed in our clinical pathology laboratory and validated at our institution was used for IHC analysis of PD-L1 expression. Briefly, 4-μm thick sections obtained from formalin-fixed, paraffin-embedded samples were stained for PD-L1 with an anti-human PD-L1 rabbit monoclonal antibody (clone SP263; Ventana, Tucson, AZ) using the automated Ventana BenchMark Ultra platform (Ventana, Tucson, AZ). Sections were counterstained with hematoxylin. PD-L1 expression was evaluated on both tumor cells and on lymphocytes and was estimated as the percentage of total tumor cells or infiltrating immune cells, respectively.

Statistical analyses were performed using Microsoft Excel (Microsoft Corporation, Redmond, Washington) and MedCalc software (MedCalc Software, Inc, Mariakerke, Belgium). Whenever possible with the available data, confidence intervals and p-values were calculated using MedCalc.

Results

Twenty-three patients diagnosed with “pure” desmoplastic primary melanoma at our institution from 1995 to 2016 were identified. Of these, tissue blocks were available for 12. Tissue from one specimen did not withstand the staining protocol on repeated attempts and so could not be evaluated. Analysis was completed on 11 patients. Four were initial biopsies and seven were excisional specimens. There was a male:female ratio of 8:3. Five (45%; 95% Confidence Interval [CI], 17 to 77%) of the tumors were located on the head and neck, with four on an upper extremity, one on the chest, and one on the great toe.

Review of the histopathology revealed that nine lesions contained an intra-epidermal component (82%; 95% CI, 48 to 98%), showing lentiginous growth with predominantly single cell growth along the junction and scattered cohesive nests. Within the dermis, the spindled cells had an infiltrative growth pattern. The edges of the lesions were difficult to define on H&E staining, but were appreciated on IHC staining with S100 antibody on a subset of cases. The desmoplastic stromal change in conjunction with the presence of spindled cells otherwise allowed for demarcation of the tumor edges. Cytologically, the dermal spindled cells ranged from small and bland to enlarged and hyperchromatic to bizarre. Mitotic figures were seen in four tumors (36%; 95% CI, 11 to 69%). The intervening stroma had a blue-grey to fibrotic appearance. Scattered loosely-arranged aggregates of mature-appearing lymphocytes were found both within and at the periphery of all of the lesions (Figure 1). Features of overt germinal center formation within the aggregates was not evident. Microscopic satellitosis, lymphovascular invasion or perineural infiltration were not identified.

Follow up data (Table 1) from our cohort revealed that one patient (1/11, 9%; 95% CI, 0 to 41%) recurred eight months after wide local excision (WLE), with tender lymph nodes in his neck that were FDG-avid on PET-CT scan. That patient was treated with neck dissection and has been without evidence of disease after two months of follow-up. Seven patients lived without disease for a mean of 84 months. Three patients succumbed to other diseases at a mean follow up time of 83 months.

The patient information and prognostic factors of the lesions are summarized in Table 1.

Review of 11 dermal scars (Table 1) revealed a variety of appearances from acutely inflamed biopsy site change to pauci-cellular fibrosis. The cancer re-excision site scars (scar patients 2, 7, 8, 10) contained a discrete epidermal defect and dermal scar with acute and chronic inflammation. Hypertrophic scars showed thickened collagen with little inflammation.

Multispectral imaging of the DM specimens on the Vectra 3.0 Pathology Imaging System revealed that immune cell aggregates in the majority of DMs contained organized aggregates of $CD20^+$ B cells surrounded by $CD8^+$ T cells, with $PNAd^+$ vessels and $CD83^+$ activated dendritic cells in the T cell zones (Figure 2). Overall, 8/11 (73%; 95% CI, 39 to 94%) DM specimens had classical TLS; representative images are shown in Figure 3. In all cases where classical TLS were present, multiple such structures were identified. Classical TLS were not identified in 3/11 cases (27%; 95% CI, 6 to 61%): one case showed all features of a TLS except B cells, and another case had no evidence of $PNAd^+$ vasculature. If broadening the definition of TLS to include both classical and non-classical structures, 10/11 (91%; 95% CI, 59 to 100%) tumors were positive for TLS. One case contained only scattered lymphocytic aggregates with no evidence of TLS formation. Features of TLS identified in our patient cohort are summarized in Table 1.

One of 12 scar samples did not withstand the repeated staining protocol for multispectral imaging; so, it was excluded from analysis. Thus, 11 scars were analyzed with multispectral imaging. TLS were absent from most of the scar specimens, but were identified in three of them (3/11, 27%; 95% CI, 6 to 61%); all three had features of classical TLS. Representative images are shown in Figure 4. Thus, while classical TLS were identified in both desmoplastic melanomas and scars, they were evident in a higher percentage of DM cases than in scar (chi-square, $p = 0.045$).

To explore whether PD-L1 expression was associated with TLS structures in DM, PD-L1 expression was assessed by IHC. Six of 11 DMs (54%; 95% CI, 23 to 83%) exhibited PD-L1 expression in ≥1% of melanoma cells (Table 1). TLS were evident in 5 of the 6 with PD-L1 expression by melanoma cells. PD-L1 expression was also identified in at least 5% of immune cells in 10 of 11 (91%) DMs and in all of the DMs with TLS (Table 1). Of the 3 DMs without TLS, PD-L1 expression was found in no more than 10% of immune cells; in contrast, it was expressed in 10–50% of immune cells in 5 of 8 tumors with TLS. In the tumors with highest PD-L1 expression in melanoma cells (DM10 60%, DM11 30%), PD-L1 expression was also high in immune cells and was densely concentrated within structures identified as TLS (Figure 5).

Discussion

DMs present diagnostic challenges. They can evade clinical detection due to their typical lack of pigment and subtle histologic findings. The presence of lymphoid aggregates in DMs is an intriguing feature. They can be seen in scars, benign melanocytic nevi [28], and even conventional melanomas [16–18]; thus, they are not strictly pathognomonic for DMs. However, these lymphoid aggregates are easily recognizable and are helpful in the histologic

identification of DMs. Their cellular composition in DM has not previously been defined, and may provide new insights about their role in the biology of the host:tumor interactions in DM. [29]

We found that these lymphoid aggregates were organized and have features of classical TLS in the majority of cases (8/11) examined. In all cases where at least one TLS was present, multiple TLS were identified. Unlike conventional melanomas, where most TIL and TLS are typically situated at the periphery of the tumor masses[8,17,30], the TLS seen in DMs were both within and around the malignant cell infiltrate. DMs carry an unusually high mutational burden, and lack the common oncogenic mutations seen in conventional melanomas such as BRAF and NRAS [19]. Their high mutational rate may contribute to production of neoantigens, and may support immune activation and immune cell infiltration into the tumors. The relationships among TLS, T cell infiltration, and Th1 immune signatures in melanoma are not fully defined, but TLS may support immune infiltration and tumor control [8]. In murine models, $PNAd^+$ lymph node-like vasculature enables CD8 effector and CD8 naive T cells to enter melanoma deposits, increasing antitumor immunity and improving prognosis [31–33]. Thus, it seems likely that the TLS in DM, which contain PNAd+ vasculature, may participate in immunologic control of cancer progression. Intriguingly, DMs show a distinct biological behavior when compared to conventional melanomas. Unlike conventional melanomas which commonly spread to regional lymph nodes, DMs rarely do [25,34,35]. Also, DM tend to be locally aggressive, although in some cases this may be due to poor delineation of margins as infiltrative DMs are so difficult to distinguish both clinically and histologically from the surrounding uninvolved stroma.

The two cases with the highest PD-L1 expression both by tumor cells and lymphocytes exhibited a localization of staining within TLS. PD-L1 expression has been associated both with IFN-γ [22] and TIL [24,36]; our study suggests that expression may be enhanced in areas of TLS formation. However, there was a wide range of PD-L1 expression by tumor cells, and higher expression by immune cells than by the melanoma cells. The high expression by immune cells suggests that there is high IFN-γ within the tumor microenvironments for most of these tumors, and especially in those with TLS. An interpretation of the data could be that this leads to high PD-L1 expression by tumor cells in a minority of tumors (DM10, DM11), but that the desmoplastic melanoma cells in other tumors may be intrinsically non-responsive to IFN-γ, either by downregulation of the IFN-γ receptor or by downregulation or mutation in JAK or STAT genes. Understanding these phenomena could help to understand the quality of the antitumor T cell response in these patients, and whether the presence of TLS, coupled with measures of tumor cell responsiveness to IFN-γ may help to identify DM patients who may respond to checkpoint blockade.

Future directions include additional investigations to define mechanisms of development of TLS within DM, not only to provide additional information pertaining to the immunobiology of the disease, but in the hope of identifying patients who may benefit from immunotherapies. Future studies should also assess why the TLS in DM tend to be intratumoral, whereas conventional melanomas commonly have them only at the periphery (invasive margin), and why the chronic infiltrate does not organize into TLS for a subset of

DMs. Other relevant questions are whether chemokine profiles differ between TLS in DM vs scar and whether T cells in the TLS are activated and antigen experienced, or naïve, and whether they differ compared to the few TLS seen in scars. As these features are elucidated, it will be valuable to understand how those findings may help to differentiate scar from residual DM at the time of DM re-excision. It will also be valuable to understand the antigens, including neoantigens, recognized by CD4 and CD8 T cells within the TLS. We hypothesize that DM with higher mutational burden may present more neoantigens and may be more likely to have TLS. A larger study would also be valuable to test associations of the presence and number of TLS in DM with survival data.

In summary, we have characterized the lymphoid aggregates of DM as TLS. They appear likely to be a part of an adaptive immune response and may be helpful for diagnosis and for understanding the immunobiology of the tumor microenvironment of DM.

Acknowledgments

Sources of funding: Rebecca Clary Harris fellowship; NIH/NCI P30 CA044579 (Cancer Center Support Grant; Biorepository and Tissue Research Facility); Department of Pathology, University of Virginia.

References

1. Lens MB, Newton-Bishop JA, Boon AP. Desmoplastic malignant melanoma: a systematic review. Br J Dermatol. 2005; 152(4):673–678. [PubMed: 15840097]
2. Jain S, Allen PW. Desmoplastic malignant melanoma and its variants: a study of 45 cases. Am J Surg Pathol. 1989; 13(5):358–373. [PubMed: 2712188]
3. Busam KJ, Mujumdar U, Hummer A, Nobrega J, Hawkins WG, Coit DG, et al. Cutaneous Desmoplastic Melanoma: Reappraisal of Morphologic Heterogeneity and Prognostic Factors. Am J Surg Pathol. 2004; 28(11):1518–1525. [PubMed: 15489657]
4. de Almeida LS, Requena L, Rutten A, Kutzner H, Garbe C, Pestana D, et al. Desmoplastic malignant melanoma: a clinicopathologic analysis of 113 cases. Am J Dermatopathol. 2008; 30(3): 207–215. [PubMed: 18496419]
5. Drayton DL, Liao S, Mounzer RH, Ruddle NH. Lymphoid organ development: from ontogeny to neogenesis. Nat Immunol. 2006; 7(4):344–353. [PubMed: 16550197]
6. Dieu-Nosjean MC, Goc J, Giraldo NA, Sautes-Fridman C, Fridman WH. Tertiary lymphoid structures in cancer and beyond. Trends Immunol. 2014; 35(11):571–580. [PubMed: 25443495]
7. Goc J, Germain C, Vo-Bourgais TK, Lupo A, Klein C, Knockaert S, et al. Dendritic cells in tumor-associated tertiary lymphoid structures license the positive prognostic value of tumor-infiltrating CD8+ T cells. Cancer Res. 2013
8. Messina JL, Fenstermacher DA, Eschrich S, Qu XT, Berglund AE, Lloyd MC, et al. 12-Chemokine Gene Signature Identifies Lymph Node-like Structures in Melanoma: Potential for Patient Selection for Immunotherapy? Scientific Reports. 2012; 2
9. Wirsing AM, Rikardsen OG, Steigen SE, Uhlin-Hansen L, Hadler-Olsen E. Characterisation and prognostic value of tertiary lymphoid structures in oral squamous cell carcinoma. BMC Clin Pathol. 2014; 14(38)
10. Engelhard VH, Rodriguez AB, Mauldin IS, Woods AN, Peske JD, Slingluff CL. Immune Cell Infiltration and Tertiary Lymphoid Structures as Determinants of Antitumor Immunity. The Journal of Immunology. 2018; 200(2):432–442. [PubMed: 29311385]
11. Neyt K, Perros F, GeurtsvanKessel CH, Hammad H, Lambrecht BN. Tertiary lymphoid organs in infection and autoimmunity. Trends in Immunology. 2012; 33(6):297–305. [PubMed: 22622061]
12. Dieu-Nosjean M, Goc J, Giraldo NA, Sautes-Fridman C, Fridman WH. Tertiary lymphoid structures in cancer and beyond. Trends in Immunology. 2014; 35(11):571–580. [PubMed: 25443495]

13. Dieu-Nosjean M, Antoine M, Danel C, Heudes D, Wislez M, Poulot V, et al. Long-Term Survival for Patients With Non–Small-Cell Lung Cancer With Intratumoral Lymphoid Structures. Journal of Clinical Oncology. 2008; 26(27):4410–4417. [PubMed: 18802153]
14. Goc J, Fridman WH, Sautes-Fridman C, Dieu-Nosjean M. Characteristics of tertiary lymphoid structures in primary cancers. OncoImmunology. 2013; 2(12):e26836. [PubMed: 24498556]
15. Ladanyi A, Kiss J, Somlai B, Gilde K, Fejos Z, Mohos A, et al. Density of DC-LAMP+ mature dendritic cells in combination with activated T lymphocytes infiltrating primary cutaneous melanoma is a strong independent prognostic factor. Cancer Immunology, Immunotherapy. 2007; 56(9):1459–1469. [PubMed: 17279413]
16. Ladanyi A, Sebestyen T, Mohos A, Liszkay G, Somlai B, Toth E, et al. Ectopic lymphoid structures in primary cutaneous melanoma. Pathol Oncol Res. 2014; 20(4):981–985. [PubMed: 24781762]
17. Mihm MC Jr, Mulé JJ. Reflections on the histopathology of tumor-infiltrating lymphocytes in melanoma and the host immune response. Cancer Immunol Res. 2015; 3(8):827–835. [PubMed: 26242760]
18. van Baren N, Baurain JF, Coulie PG. Lymphoid neogenesis in melanoma: what does it tell us. OncoImmunology. 2013; 2(1)
19. Shain AH, Garrido M, Botton T, Talevich E, Yeh I, Sanborn JZ, et al. Exome sequencing of desmoplastic melanoma identifies recurrent NFKBIE promoter mutations and diverse activating mutations in the MAPK pathway. Nature genetics. 2015; 47(10):1194–1199. [PubMed: 26343386]
20. Rabbie R, Adams DJ. Desmoplastic melanoma: C>Ts and NF-κB. Pigment Cell & Melanoma Research. 2016; 29(2):120–121. [PubMed: 26663830]
21. Frydenlund N, Leone D, Yang S, Hoang MP, Deng A, Hernandez-Perez M, et al. Tumoral PD-L1 expression in desmoplastic melanoma is associated with depth of invasion, tumor-infiltrating CD8 cytotoxic lymphocytes and the mixed cytomorphological variant. Modern Pathology. 2017
22. Spranger S, Bao R, Gajewski TF. Melanoma-intrinsic beta-catenin signalling prevents anti-tumour immunity. Nature. 2015; 523(7559):231–235. [PubMed: 25970248]
23. Kaunitz GJ, Cottrell TR, Lilo M, Muthappan V, Esandrio J, Berry S, et al. Melanoma subtypes demonstrate distinct PD-L1 expression profiles. Laboratory Investigation. 2017; 97(9) labinvest201764.
24. Obeid JM, Erdag G, Smolkin ME, Deacon DH, Patterson JW, Chen L, et al. PD-L1, PD-L2 and PD-1 expression in metastatic melanoma: Correlation with tumor-infiltrating immune cells and clinical outcome. Oncoimmunology. 2016; 5(11):e1235107. [PubMed: 27999753]
25. George E, McClain SE, Slingluff CL, Polissar NL, Patterson JW. Subclassification of desmoplastic melanoma: pure and mixed variants have significantly different capacities for lymph node metastasis. J Cutan Pathol. 2009; 36(4):425–432. [PubMed: 19278427]
26. Busam KJ. Cuatneous desmoplastic melanoma. Adv Anat Pathol. 2005; 12(2):92–102. [PubMed: 15731577]
27. Hawkins WG, Busam KJ, Ben-Porat L, Panageas KS, Coit DG, Gyorki DE, et al. Desmoplastic melanoma: a pathologically and clinically distinct form of cutaneous melanoma. Ann Surg Oncol. 2005; 12(3):207–213. [PubMed: 15827812]
28. Kiuru M, Patel RM, Busam KJ. Desmoplastic melanocytic nevi with lymphocytic aggregates. J Cutan Pathol. 2012; (39):940–944. [PubMed: 22845683]
29. Kraft S, Fernandez-Figueras M-T, Richarz NA, Flaherty KT, Hoang MP. PDL1 expression in desmoplastic melanoma is associated with tumor aggressiveness and progression. Journal of the American Academy of Dermatology. 2017; 77(3):534–542. [PubMed: 28728868]
30. Cipponi A, Mercier M, Seremet T, Baurain JF, Theate I, van den Oord J, et al. Neogenesis of lymphoid structures and antibody responses occur in human melanoma metastases. Cancer Research. 2012; 72(16):3997–4007. [PubMed: 22850419]
31. Peske JD, Thompson ED, Gemta L, Baylis RA, Fu YX, Engelhard VH. Effector lymphocyte-induced lymph node-like vasculature enables naive T-cell entry into tumours and enhanced anti-tumour immunity. Nature communications. 2015; 6:7114.

32. Peske JD, Woods AB, Engelhard VH. Control of CD8 T-Cell Infiltration into Tumors by Vasculature and Microenvironment. Advances in cancer research. 2015; 128:263–307. [PubMed: 26216636]

33. Brinkman CC, Peske JD, Engelhard VH. Peripheral tissue homing receptor control of naive, effector, and memory CD8 T cell localization in lymphoid and non-lymphoid tissues. Front Immunol. 2013; 4:241. [PubMed: 23966998]

34. Gyorki DE, et al. Sentinel lymph node biopsy for patients with cutaneous desmoplastic melanoma. Annals of Surgical Oncology. 2003; 10:403. [PubMed: 12734089]

35. Pawlik TM, Ross MI, Prieto VG, et al. Assessment of the role of sentinel lymph node biopsy for primary cutaneous desmoplastic melanoma. Cancer. 2006; (106):900. [PubMed: 16411225]

36. Kaunitz GJ, Cottrell TR, Lilo M, Muthappan V, Esandrio J, Berry S, et al. Melanoma subtypes demonstrate distinct PD-L1 expression profiles. Laboratory investigation; a journal of technical methods and pathology. 2017; 97(9):1063–1071. [PubMed: 28737763]

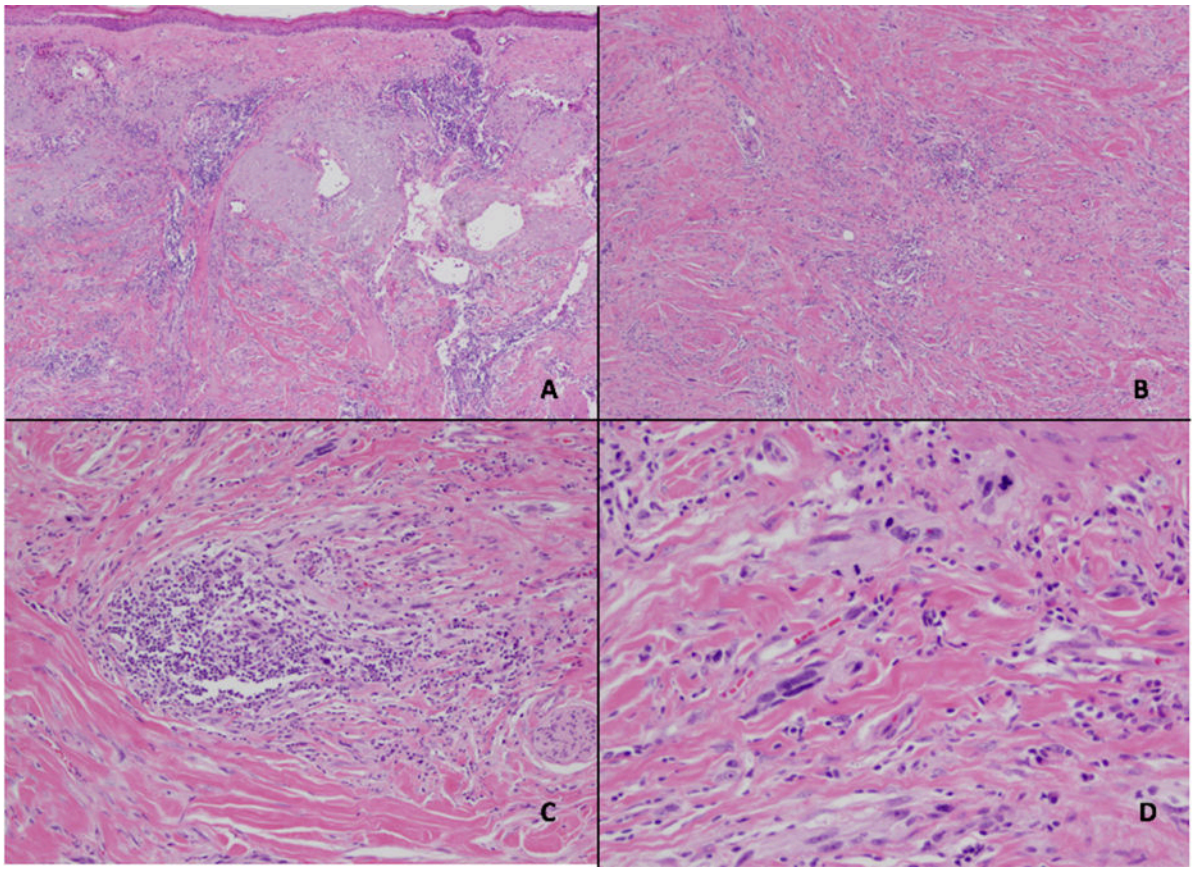

Figure 1.

Desmoplastic melanoma. Microscopic images of a desmoplastic melanoma excision showing a low-power view of an effaced epidermis overlying sun-damaged skin containing an invasive, infiltrative spindle cell proliferation with scattered intratumoral lymphoid aggregates (A, H&E 2x). Deep within the dermis, the spindled melanocytes are seen within a desmoplastic stroma (B, H&E 4x) with scattered lymphoid aggregates among the malignant cells (C, H&E 10x). Cytologically, the melanocytes display significant pleomorphism and mitotic activity (D, H&E 20x).

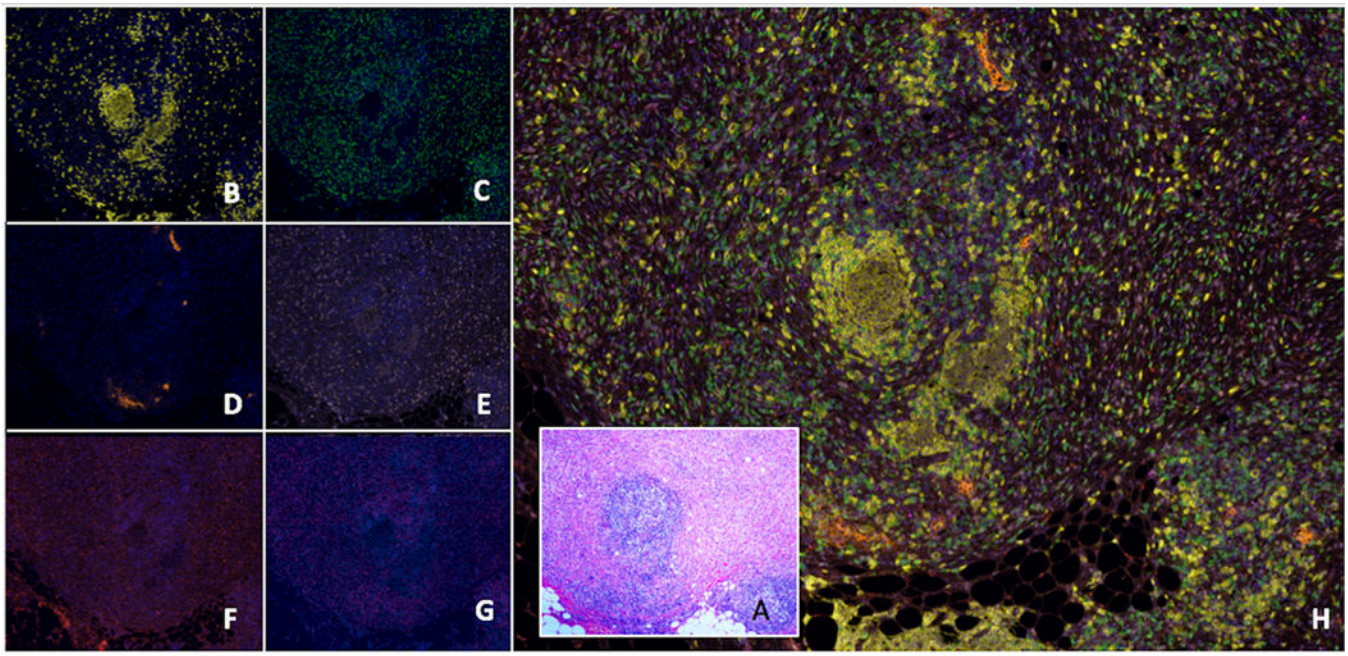

Figure 2.

A representative tertiary lymphoid structure (TLS) identified in desmoplastic melanoma (DM) seen by hematoxylin and eosin (H&E) and multispectral immunofluorescent staining. (A) A routine stained section of DM invading to the subcutaneous adipose tissue (A, H&E, 2X). An intratumoral lymphoid aggregate is evident near the center of the image, which is detailed in images B–H. Other peritumoral lymphoid aggregates are also evident at the tumor margin invading fat on the inferior aspect of the image. Spectrally unmixed images (20x) of the corresponding section are shown including: (B) A follicle of CD20+ B cells (yellow); (C) CD8+ T cells (green) surrounding the B cell center; (D) PNAd+ vasculature (orange) adjacent to the B-cell zones; (E) Ki67 (light pink) marker highlighting proliferating lymphoid cells but also tumor cells; (F) CD83+ activated dendritic cells (red) predominantly in the T cell zone; (G) FoxP3 (magenta) staining scattered cells. (H) A composite image highlighting all the markers studied composing a well-formed TLS.

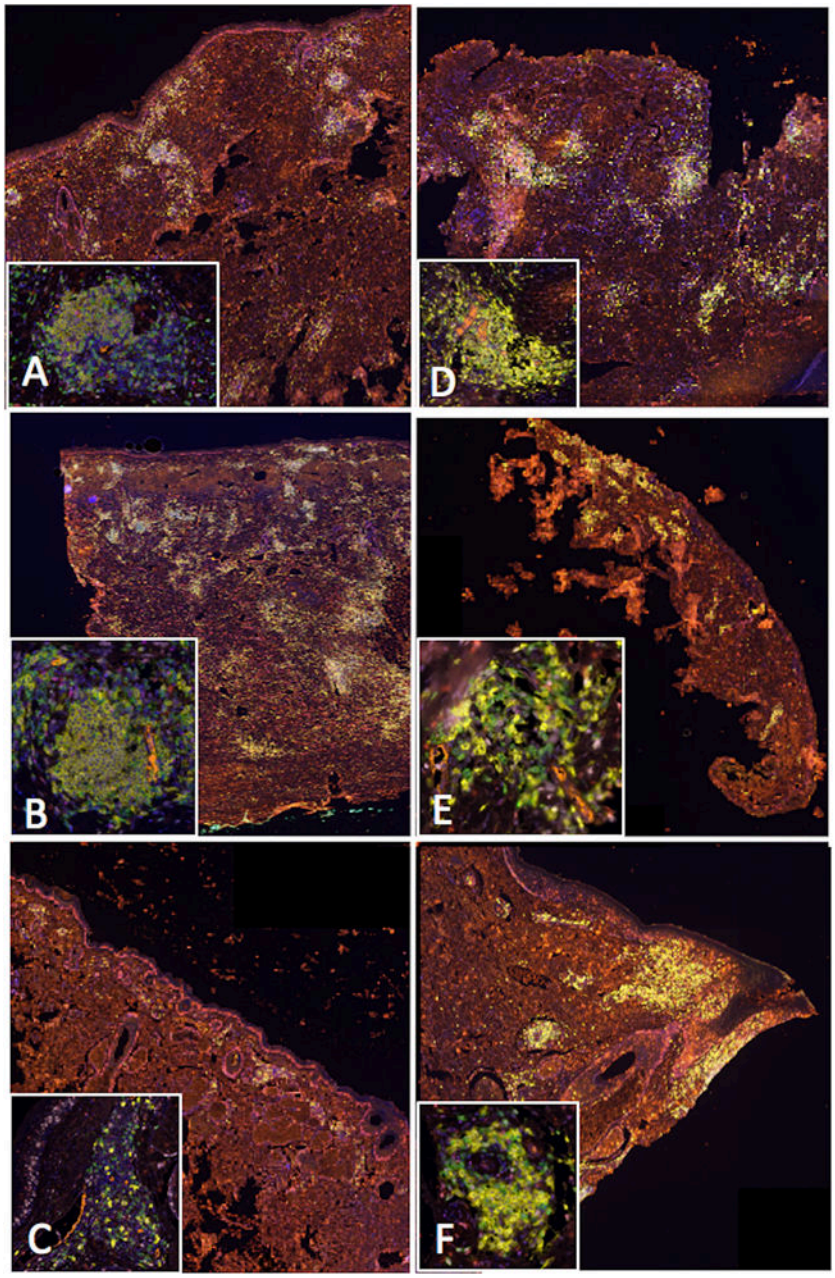

Figure 3.

Multispectral immunofluorescent, spectrally unmixed, composite images of classical TLS identified in DM cases (10x). Brightly staining areas are TLS visualized at low-power throughout the dermis. Inset images display a high-power view of a single TLS (20x). Key: CD20+ (B cells) = yellow; CD8+ (T cells) = green; PNAd+ (HEVs) = orange; CD83+ (activated dendritic cells) = red; Ki67+ (proliferation marker) = light pink; FoxP3+ (T regs) = magenta; DAPI (nuclear counterstain) = blue. In all these images, the biopsies are comprised almost completely of the desmoplastic melanoma, and all the TLS in the insets are within the tumors, rather than at invasive margins.

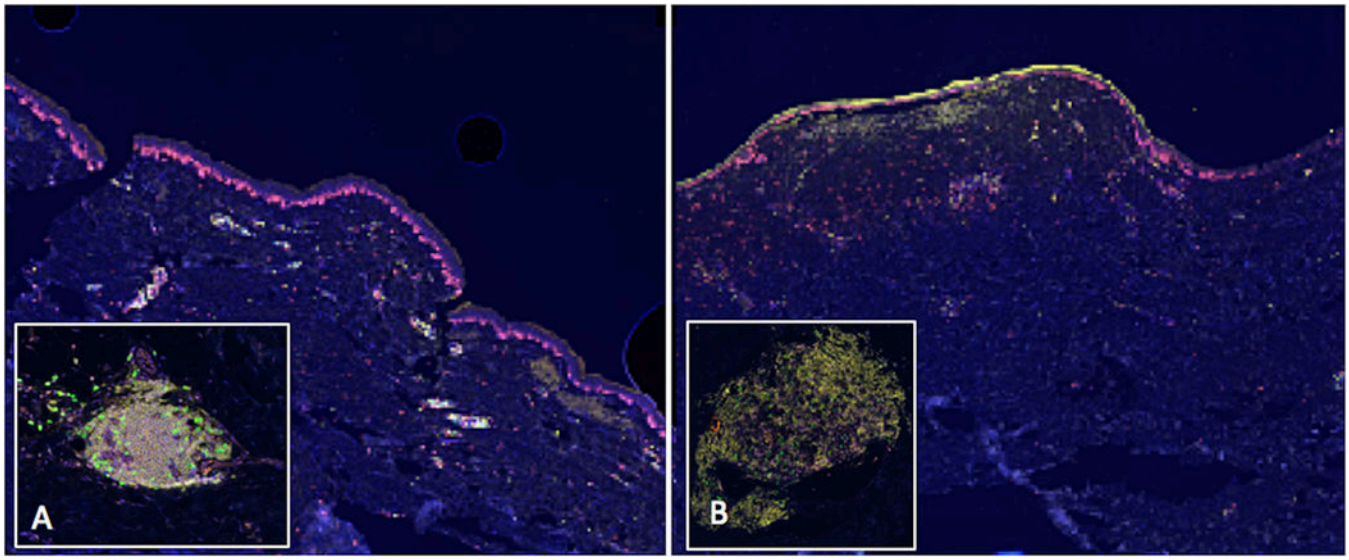

Figure 4.

Tertiary lymphoid structures (TLS) identified in scars by multispectral immunofluorescence imaging (spectrally unmixed, 20x). Low-power images show the brightly staining lymphoid aggregates in the papillary dermis. Inset images highlight a single TLS. (A) A hypertrophic scar collected from an excision of an atypical melanocytic lesion. (B) A scar excised from the site of a junctional nevus with melanocytic hyperplasia.

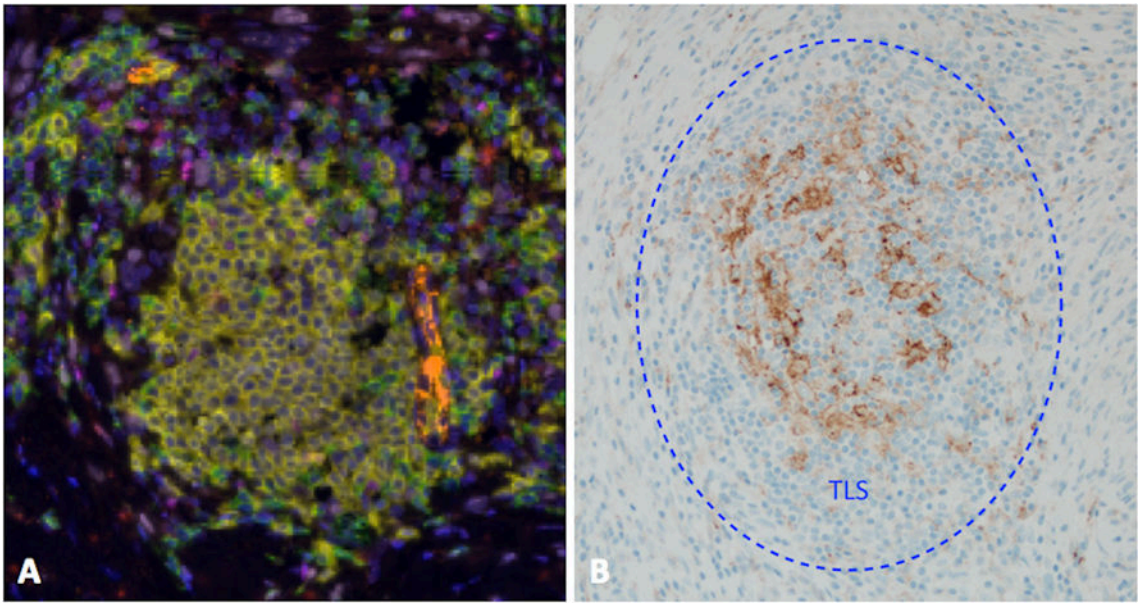

Figure 5.

Pronounced localization of PD-L1 expression within a TLS in a case of DM that exhibited expression of PD-L1 by 30% tumor cells and 50% immune cells. (A) A representative intratumoral TLS. Many such structures were identified throughout this specimen. Key: CD20+ (B cells) = yellow; CD8+ (T cells) = green; PNAd+ (HEVs) = orange; CD83+ (activated dendritic cells) = red; Ki67+ (proliferation marker) = light pink; FoxP3+ (T regs) = magenta; DAPI (nuclear counterstain) = blue. (B) PDL1 expression localized to cells within identified TLS.

Table 1

Patient demographics, tumor prognostic features, follow up data, TLS status, and PD-L1 expression in patients with primary desmoplastic melanomas (DM1-DM11) and with scar (S1–S11). MIS = melanoma in situ; SCCa = squamous cell cancer; BCCa = basal cell cancer, ANED = Alive with no evidence of disease; DOC = dead from other causes; N/A = not applicable; ND = not done.

Sample	Age/ Sex	Site	Procedure	Breslow (mm)/ Clark level	Clark level	Ulceration	Mitoses per mm2	LVSI/PNI	Clinical IHC	SLN	Follow Up (Mos)	Current Status	TLS	PD-L1 expression (%)	
														tumor cells	immune cells
DM1	68/M	Arm	Biopsy	2.7	IV	ND	5	ND	ND	Neg	143	ANED	Classical	< 1%	5 – 10%
DM2	66/M	Cheek	Excision	3.4	V	ND	0	ND	ND	ND	194	ANED	Classical	< 1%	5%
DM3	55/F	Arm	Biopsy	1.2	IV	ND	ND	ND	ND	ND	208	DOC	Absent	< 1%	< 5%
DM4	55/F	Arm	Biopsy	5.0	V	ND	ND	ND	ND	Neg	71	ANED	Classical	1 – 5%	30 – 40%
DM5	61/M	Toe	Excision	10.0	V	Yes	0	No	ND	Neg	137	ANED	Classical	< 1%	10%
DM6	74/M	Arm	Excision	12.5	V	No	1	PNI	S100+ Melan-A-HMB-45-	Neg	25	DOC	Non-classical (no B cells)	5%	5%
DM7	64/M	Chest	Biopsy	1.8	IV	No	0	No	S100+	ND	30	ANED	Classical	1%	5 – 10%
DM8	>85/M	Scalp	Excision	1.3	ND	ND	ND	ND	S100+	ND	16	DOC	Non-classical (no PNAd+ HEV)	< 1%	5 – 10%
DM9	72/M	Scalp	Excision	4.4	ND	ND	ND	ND	S100+	Neg	0	ANED	Classical	1%	30 – 40%
DM10	68/M	Scalp	Re-excision	9.2	V	No	7	PNI	SOX10+	ND	8	Recurred	Classical	60%	30 – 40%
DM11	70/F	Neck	Excision	20.8	V	No	2	PNI	ND	Neg	11	ANED	Classical	30%	50%
S1	62/M	Abdominal wall	Excision at repair of recurrent hernia	N/A	N/A	N/A	N/A	N/A	N/A	N/A	20	N/A	Absent	ND	ND
S2	45/M	Foot	Re-excision of MIS	N/A	N/A	N/A	N/A	N/A	N/A	N/A	6	N/A	Absent	ND	ND
S3	74/M	Forehead	Excision, Scar revision	N/A	N/A	N/A	N/A	N/A	N/A	N/A	15	N/A	Classical	ND	ND
S4	58/M	Arm	Re-excision of SCCa	N/A	N/A	N/A	N/A	N/A	N/A	N/A	1	N/A	Absent	ND	ND
S5	42/M	Abdominal wall	Excision, repair of chronic wound	N/A	N/A	N/A	N/A	N/A	N/A	N/A	252	N/A	Absent	ND	ND
S6	75/F	Cheek	Excision at scar revision	N/A	N/A	N/A	N/A	N/A	N/A	N/A	10	N/A	Classical	ND	ND
S7	40/F	Scalp	Re-excision of recurrent BCCa	N/A	N/A	N/A	N/A	N/A	N/A	N/A	49	N/A	Absent	ND	ND
S8	78/M	Back	Wide excision melanoma	N/A	N/A	N/A	N/A	N/A	N/A	N/A	1	N/A	Classical	ND	ND
S9	71/M	Back	Excision of residual atypical nevus	N/A	N/A	N/A	N/A	N/A	N/A	N/A	1	N/A	Absent	ND	ND
S10	>85/M	Back	Re-excision of MIS	N/A	N/A	N/A	N/A	N/A	N/A	N/A	1	N/A	Absent	ND	ND
S11	62/F	Shoulder	Excision of suspicious papule	N/A	N/A	N/A	N/A	N/A	N/A	N/A	0	N/A	Absent	ND	ND